ARTICLE

Analysis of Single-Walled Carbon Nanotubes Using a Chemical Bond Element Model

Ji-nan Lu, Hai-bo Chen*

Department of Modern Mechanics, University of Science and Technology of China, Hefei 230027, China
Key Laboratory of Mechanical Behavior and Design of Materials, Chinese Academy of Sciences, Hefei 230027, China

(Dated: Received on January 25, 2008; Accepted on May 16, 2008)

A three dimensional nano-scale finite element model (FEM), called the chemical bond element model, is proposed for the simulation of mechanical properties of single-walled carbon nanotubes (SWCNTs) based upon molecular mechanics method. Chemical bonds between carbon atoms are modeled by chemical bond elements. The constants of a sub-stiffness matrix are determined by using a linkage between molecular mechanics and continuum mechanics. In order to evaluate the correctness and performance of the proposed model, simulation was done to determine the influence of nanotube wall thickness, radius and length on the elastic modulus (Young's modulus and shear modulus) of SWCNTs. The simulation results show that the choice of wall thickness significantly affects the Young's modulus and shear modulus. The force field constants is also very important, because the elastic modulus is sensitive to force field constants and the elastic properties of SWCNT are related to the radii of the tubes. The contribution of length to elastic modulus is insignificant and can be ignored. In comparison with the Young's modulus and shear modulus reported in the literature, the presented results agree very well with the corresponding theoretical results and many experimental measurements. Furthermore, if the force constants are properly chosen, the present method could be conveniently used to predict the mechanical behavior of other single-walled nanotubes such as boron nitride nanotubes. The results demonstrate the value of the proposed model as a valuable tool in the study of mechanical behaviors of carbon nanotubes and in the analysis of nanotube-based equipments.

Key words: Single-walled carbon nanotube, Finite element method, Elastic property, Molecular mechanics

I. INTRODUCTION

Ever since their discovery [1], carbon nanotubes have been recognized as particularly important nanoscopic systems [2,3]. The mechanical properties of CNTs have been determined by a number of experiments [4-8]. So far, a number of simulation methods have been developed to investigate the behaviors of nanotubes. Molecular dynamics (MD) is perhaps the most popular method currently employed for nano-scale analysis. It has been employed to calculate modulus and strength for polymer [9,10], nanotube [11,12], and nanotube reinforced polymer. However, the frequency of molecular thermal vibration is so high that, the deformations which MD simulation provide can only occur on the too-short time scale of maybe nano-seconds.

Monte Carlo simulation is another method based upon statistical theory and it has been employed to investigate nano-scale polymer deformation [13,14]. To assure the accuracy, the speed of the convergence of the process must be slow, quite similar to MD method, thus the Monte Carlo method could not obtain deformation information unless within a transitory time scale and strain rates used ranged from 108/s to 109/s. For most engineering problems, the high frequency of thermal dynamic molecular motion does not affect elastic deformation, material modulus remains approximately constant within a large temperature range which contradicts the hyper strain rates in MD and Monte Carlo methods. Though Theodorou and Suter performed a detailed theoretical study of how to decouple the elastic response of materials from the high frequency of thermal dynamical vibration in a molecular computational model [15], there are still some drawbacks in their work.

Li and Chou successfully developed a continuum mechanics model for mechanical properties of nanotubes by linking the molecular mechanics constants of force fields and frame sectional stiffness parameters [16]. Size-dependent Young's modulus and shear modulus of armchair and zigzag nanotubes have been predicted. This kind of method is adopted and used by many scholars for simulations, associated with finite element method. Cho [17], Tserpes and Papanikos [18], Kalamkarov *et al.* [19], Meo and Rossi [20], Kirtania and Chakraborty [21] analyzed the elastic properties of SWCNTs. Chang and Gao developed an analytical molecular mechanics model to relate the elastic properties of a single-walled carbon nanotubes (SWCNTs) to its atomic structure with calibrated force field constants [22]. Based on a link between molecular and solid mechanics, Toshiaki Natsuki *et al.* used an analytical method for modeling the elastic properties of SWCNTs [23]. After that, Xiao *et al.* and Chang *et al.* systemat-

*Author to whom correspondence should be addressed. E-mail: hbchen@ustc.edu.cn, Tel.: +86-551-3603724

ically analyzed the attributions of chirality and size of nanotubes to elastic properties of SWCNTs with analytical molecular mechanics model [24,25]. Huang *et al.* and Lu *et al.* used a special method to decompose the transfiguration energy of SWCNTs and under equivalent discrete energy models, the Young's modulus and properties of dynamics of SWCNTs have been reported [33,34].

In this work, a new chemical bond element model is developed and employed to simulate the mechanical properties of SWCNT. When SWCNT is subjected to loadings, it behaves like space-frame structures but the sub-stiffness matrix is not the same as the macroscopic beam. The sub-stiffness matrix is obtained by using a linkage between molecular mechanics and continuum mechanics. The three dimensional (3D) chemical bond element stiffness matrices are deduced and formulated. The determination of Young's modulus, shear modulus and Poisson's ratio of SWCNTs were focused on. For its simplicity and less restrictions (shape and boundary condition restrictions), the proposed model can be further applied in the simulations of nano-scale equipments.

II. MOLECULAR MECHANICS METHOD

From the viewpoint of molecular mechanics, the general expression of total steric potential energy is a sum of energies due to valence or bonded interactions and non-bonded interactions [27]:

$$E_{\rm t} = U_r + U_\theta + U_\varphi + U_\omega + U_{\rm Vdw} + U_{\rm es} \tag{1}$$

where U_r is associated with bond stretch interaction, U_θ with bond angle bending, U_φ with dihedral angle torsion, U_ω with bond angle inversion, $U_{\rm Vdw}$ with non-bonded van der Waals interaction, and $U_{\rm es}$ with electrostatic force interaction. $U_{\rm Vdw}$ and $U_{\rm es}$ are much smaller than the former four terms, so they are usually neglected. In a three-dimensional numerical model, the bond stretch, bond angle bending and dihedral angle torsion require further consideration. In our model, the U_τ is considered to be an adjustable potential energy which involves the contribution of U_φ and U_ω.

The simplest and most extensive applied forms that relate to bond stretch of the deformation potential energies are the harmonic functions:

$$U_r = \frac{1}{2}\sum_i k_r(\Delta r_i)^2 \tag{2}$$

The relationship between restoration force and bond elongation can be derived as:

$$F_r = k_r(r - r_0) \tag{3}$$

where r_0 is the equilibrium bond length.

The harmonic potential energy function describing the angle bends interaction between two neighboring chemical bending is given as:

$$U_\theta = \frac{1}{2}\sum_j k_\theta(\Delta\theta_j)^2 \tag{4}$$

The relationship between bending moment and bending angle can be written as:

$$M_\theta = k_\theta(\theta - \theta_0) \tag{5}$$

where θ_0 is the equilibrium bond angle.

The out-of-plane torsion is expressed as:

$$\begin{aligned} U_\tau &= U_\varphi + U_\omega \\ &= \frac{1}{2}\sum_j k_\tau(\Delta\varphi_j)^2 \end{aligned} \tag{6}$$

where k_r, k_θ, and k_τ are taken to be as 742 nN/nm, 1.42 (nN·nm)/rad^2 [22], and 0.15 (nN·nm)/rad^2 [38], respectively, in this work. There is another set of constants of force field which is adopted by other researchers such as Li and Chou [16], where k_r, k_θ, and k_τ are 652 nN/nm, 0.876 (nN·nm)/rad^2, and 0.278 (nN·nm)/rad^2, respectively. The constants of force field are related to the temperature of environment theoretically, and we can employ the force field constants under different temperature throughout the testing to reflect the effect of temperature on the mechanical behaviors.

III. FORMING THREE-DIMENSIONAL CHEMICAL BOND ELEMENT MATRIX

Based on the restoration force and moment, each C−C bond is treated as a separate bond element, similar to the sub-element in the finite element method [28]. The stiffness of the bond element can be divided up to three independent segments: stretching, bending and torsion stiffness.

The stretching stiffness of the chemical bond element is determined by the relationship between restoration force and bond elongation of the distance between the two adjacent atoms, which is determined by Eq.(3). The bending stiffness of the covalent bond is determined by Eq.(5). The out-of-torsion energy of the covalent bond is so complex that here it is considered as an adjustable parameter, supposing it can be viewed as the function of Eq.(6).

Chemical bond element nodal forces and displacements are shown in Fig.1. There are six nodal forces for each node: N_{ix}, Q_{iy}, Q_{iz}, M_{ix}, M_{iy}, and M_{iz} for node i; N_{jx}, Q_{jy}, Q_{jz}, M_{jx}, M_{jy}, and M_{jz} for node j. There are six nodal displacements for each node: u_i, v_i, w_i, θ_{ix}, θ_{iy}, and θ_{iz} for node i; u_j, v_j, w_j, θ_{jx}, θ_{jy}, and θ_{jz} for node j. Quite different from traditional proposal when using strength of materials in the finite element method, the nodal degrees have some restrictions

DOI:10.1088/1674-0068/21/04/353-360

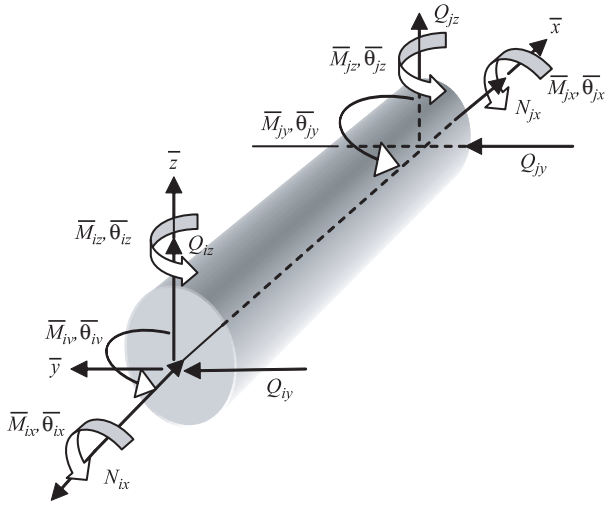

FIG. 1 Nodal forces and nodal degrees.

as shown in Fig.2. The displacements in y-direction (v_i and v_j) in the local coordinate system of two adjacent atoms are not independent, the restrictions formula are shown below.

The restriction is expressed in a function as:

$$\Delta\theta_{Lz} = \theta_{iz} - \theta_{jz} = \frac{\nu_j - \nu_i}{L} \tag{7}$$

Similar to the condition in the x-y plane, the restriction in the x-z plane is :

$$\Delta\theta_{Ly} = \frac{w_j - w_i}{L} \tag{8}$$

where L is the length of the C−C bond element. Based upon static equilibrium conditions, nodal force increments in the x-y plane and x-z plane are derived:

$$\begin{aligned} Q_{iy} &= \frac{M_{iy} + M_{jy}}{L} \\ Q_{jy} &= -\frac{M_{iy} + M_{jy}}{L} \\ Q_{iz} &= \frac{M_{iz} + M_{jz}}{L} \\ Q_{jz} &= -\frac{M_{iz} + M_{jz}}{L} \end{aligned} \tag{9}$$

where M_{iy}, M_{jy}, M_{iz}, and M_{jz} can be expressed as:

$$\begin{aligned} M_{iy} &= -2k_\theta(\Delta\theta_{Ly} - \theta_{iy}) \\ M_{jy} &= 2k_\theta(\theta_{jy} - \Delta\theta_{Ly}) \\ M_{iz} &= -2k_\theta(\Delta\theta_{Lz} - \theta_{iz}) \\ M_{jz} &= 2k_\theta(\theta_{jz} - \Delta\theta_{Lz}) \end{aligned} \tag{10}$$

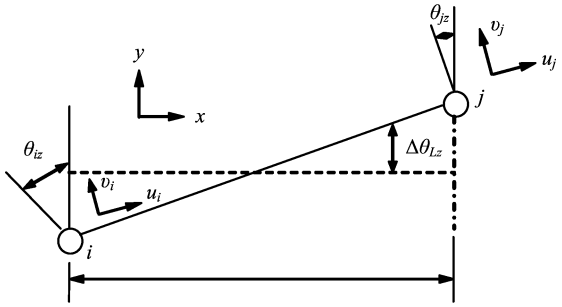

FIG. 2 Relationship between displacement and rotation angle.

Based on the formulations above, the relationships between nodal force and displacements are derived:

$$\begin{aligned} N_{ix} &= k_r u_i - k_r u_j \\ Q_{iy} &= \frac{4k_\theta}{L^2}\nu_i + \frac{2k_\theta}{L}\theta_{iz} - \frac{4k_\theta}{L^2}\nu_j + \frac{2k_\theta}{L}\theta_{jz} \\ Q_{iz} &= \frac{4k_\theta}{L^2}w_i - \frac{2k_\theta}{L}\theta_{iy} - \frac{4k_\theta}{L^2}w_j - \frac{2k_\theta}{L}\theta_{jy} \\ M_{ix} &= k_\tau\theta_{ix} - k_\tau\theta_{jx} \\ M_{iy} &= -\frac{2k_\theta}{L}w_i + 2k_\theta\theta_{iy} + \frac{2k_\theta}{L}w_j \\ M_{iz} &= \frac{2k_\theta}{L}v_i + 2k_\theta\theta_{iz} - \frac{2k_\theta}{L}v_j \\ N_{jx} &= -k_r u_i + k_r u_j \\ Q_{jy} &= -\frac{4k_\theta}{L^2}\nu_i - \frac{2k_\theta}{L}\theta_{iz} + \frac{4k_\theta}{L^2}\nu_j - \frac{2k_\theta}{L}\theta_{jz} \\ Q_{jz} &= -\frac{4k_\theta}{L^2}w_i + \frac{2k_\theta}{L}\theta_{jy} + \frac{4k_\theta}{L^2}w_j + \frac{2k_\theta}{L}\theta_{jy} \\ M_{jx} &= -k_\tau\theta_{ix} + k_\tau\theta_{jx} \\ M_{jy} &= -\frac{2k_\theta}{L}w_i + \frac{2k_\theta}{L}w_j + 2k_\theta\theta_{jy} \\ M_{jz} &= \frac{2k_\theta}{L}v_i - \frac{2k_\theta}{L}v_j + 2k_\theta\theta_{jz} \end{aligned} \tag{11}$$

The element equilibrium equation can be written as follows:

$$[K^e]\{d^e\} = \{p^e\} \tag{12}$$

where

$$\begin{aligned} \{d^e\} &= \{u_i, v_i, \omega_i, \theta_{ix}, \theta_{iy}, \theta_{iz}, u_j, v_j, \omega_j, \theta_{jx}, \theta_{jy}, \theta_{jz}\}^T \\ \{p^e\} &= \{N_{ix}, Q_{iy}, Q_{iz}, M_{ix}, M_{iy}, M_{iz}, N_{jx}, \\ &\quad Q_{jy}, Q_{jz}, M_{jx}, M_{jy}, M_{jz}\}^T \end{aligned} \tag{13}$$

K^e, the element stiffness matrix is written as:

DOI:10.1088/1674-0068/21/04/353-360

$$K^e=\begin{vmatrix}
k_r & 0 & 0 & 0 & 0 & 0 & -k_r & 0 & 0 & 0 & 0 & 0 \\
0 & \frac{4k_\theta}{L^2} & 0 & 0 & 0 & \frac{2k_\theta}{L} & 0 & -\frac{4k_\theta}{L^2} & 0 & 0 & 0 & \frac{2k_\theta}{L} \\
0 & 0 & \frac{4k_\theta}{L^2} & 0 & -\frac{2k_\theta}{L} & 0 & 0 & 0 & -\frac{4k_\theta}{L^2} & 0 & -\frac{2k_\theta}{L} & 0 \\
0 & 0 & 0 & k_\tau & 0 & 0 & 0 & 0 & 0 & -k_\tau & 0 & 0 \\
0 & 0 & -\frac{2k_\theta}{L} & 0 & 2k_\theta & 0 & 0 & 0 & \frac{2k_\theta}{L} & 0 & 0 & 0 \\
0 & \frac{2k_\theta}{L} & 0 & 0 & 0 & 2k_\theta & 0 & -\frac{2k_\theta}{L} & 0 & 0 & 0 & 0 \\
-k_r & 0 & 0 & 0 & 0 & 0 & k_r & 0 & 0 & 0 & 0 & 0 \\
0 & -\frac{4k_\theta}{L^2} & 0 & 0 & 0 & -\frac{2k_\theta}{L} & 0 & \frac{4k_\theta}{L^2} & 0 & 0 & 0 & -\frac{2k_\theta}{L} \\
0 & 0 & -\frac{4k_\theta}{L^2} & 0 & \frac{2k_\theta}{L} & 0 & 0 & 0 & \frac{4k_\theta}{L^2} & 0 & \frac{2k_\theta}{L} & 0 \\
0 & 0 & 0 & -k_\tau & 0 & 0 & 0 & 0 & 0 & k_\tau & 0 & 0 \\
0 & 0 & -\frac{2k_\theta}{L} & 0 & 0 & 0 & 0 & 0 & \frac{2k_\theta}{L} & 0 & 2k_\theta & 0 \\
0 & \frac{2k_\theta}{L} & 0 & 0 & 0 & 0 & 0 & -\frac{2k_\theta}{L} & 0 & 0 & 0 & 2k_\theta
\end{vmatrix} \quad (14)$$

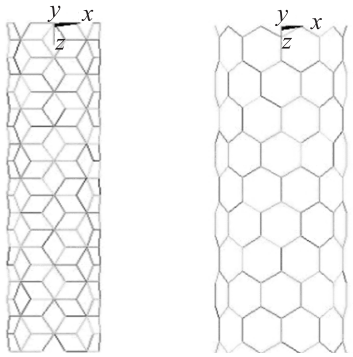

(4,4) (10,0)

FIG. 3 Side views of the FE meshes of (4,4), (10,0) SWCNT.

IV. FINITE ELEMENT APPROACH TO MODELING

Our method can be efficiently implemented by self-compiled or commercial FEM programs. In our simulation experiments, we adopted the commercial FEM software ANSYS to realize our chemical bond element method. ANSYS supplied a kind of element called MATRIX27 through which the stiffness matrix parameters is allowed to be self-defined by the users. Based on the study above, using this element, the sub-stiffness matrix of C−C bond element derived from the theoretical analysis shown by Eq.(14) can be used to form the nanotube-structure stiffness matrix in the FEM software. But ANSYS does not support the auto-transition of the stiffness matrix of MATRIX27, so we did it through matrix operation commands to realize it in our program. In this proposal, the simulation of nanotube structure links the microstructure characters presented by molecular mechanics to the continuum mechanics method: FE method.

In our calculation examples, the fixed-free SWCNT is modeled using ANSYS 11.0. It is allowed to utilize non-international units in ANSYS as long as the units are self-uniform. A proper set of units must be carefully selected otherwise the stiffness matrix of the element will be singular. If the unit of force is adopted as 0.1 nN and the unit of distance is 0.1 nm, the singularity will be avoided. In Fig.3, the side views of the FE meshes of an armchair and a zigzag SWCNT are displayed.

V. RESULTS AND DISCUSSION

In the analysis below, the reliability and efficiency of the 3D chemical bond elements method is verified. Some of the basic mechanical elastic properties of SWCNTs such as Young's modulus, shear modulus and Poisson's ratio are calculated in our model to compare with the existing theoretical and experimental results. In our model, the initial carbon-carbon bond length is taken as 142.1 pm. SWCNT has 100 layers of carbon atoms, that is to say, for armchair the length of the SWCNT is about 12.346 nm and for zigzag about 10.658 nm, and the bottom layers are fixed. The axial forces and shear forces act on each atom in the 100th layer of the model. The boundary and loading conditions on the FE models of typical SWCNTs are illustrated in Fig.4.

DOI:10.1088/1674-0068/21/04/353-360

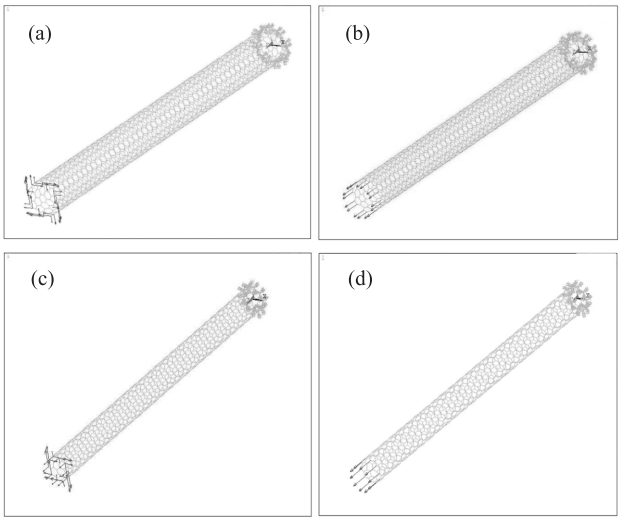

FIG. 4 Boundary and loading conditions on the FE models of typical SWCNTs. (a) Armchair (8,8), under torsion B.C., (b) Armchair (8,8), under stretching B.C., (c) Zigzag (10,0) under torsion B.C., and (d) Zigzag (10,0), under stretching B.C..

A. Young's modulus of a single-walled carbon nanotube

Two main types of carbon nanotubes, i.e., armchair and zigzag, are considered in our model. The formula in strength of materials to calculate Young's modulus is adopted which uses strain and stress to define the Young's modulus. In our model, the structure does not have thickness so we have to define an equivalent thickness of SWCNT to calculate the stress. The well-recognized thickness of SWCNT 0.34 nm is adopted in our simulations.

The variations of the calculated Young's modulus with respect to nanotube radius are plotted in Fig.5. The results show that for armchair nanotubes the Young's modulus seems to be insensitive to the variation of radius but it is sensitive for zigzag nanotubes. The Young's modulus of the zigzag nanotube increases with the radius and the convergent value of both armchair and zigzag nanotubes is about 0.881 TPa. As for the uncertainty of the thickness of SWCNT, if the product of Young's modulus and the thickness of SWCNT are considered as a modulus, then the new value is about 0.30 TPa·nm.

Besides, the calculated results using another force field constants adopted by Li and Chou are also plotted in Fig.5 [16]. From the results, the Young's modulus of SWCNT is sensitive to the force field constants in molecular mechanics method.

Our computational results are comparable to the theoretical results provided by other modeling techniques. The existing tight-binding methods showed significant scattering in predicting Young's modulus, ranging from 0.23 TPa·nm (Molina *et al.*, [39]) to 0.43 TPa·nm (Goze *et al.*, [26]). Based on a force-constant model, Lu calculated Young's modulus to be about 0.33 TPa·nm [11]. Popov *et al.* obtained the Young's modulus of SWCNTs of about 1 TPa by using the empirical lattice dynamics model [29]. It is not surprising that there exist some differences between the values given by different methods, because different parameters are used in different theories or algorithms. For instance, molecular dynamics simulations based on the Tersoff-Brenner potential by Yakobson *et al.* showed surface Young's modulus of carbon nanotube to be about 0.36 TPa·nm [30], while molecular dynamics results based on the Keating potential by Overney *et al.* produce a value of about 0.51 TPa·nm [31]. By a non-orthogonal tight-binding molecular dynamics simulation, Hernandez *et al.* revealed the dependency of the Young's modulus on nanotube radius and chirality and gave an average value of 1.24 TPa [32]. Based on molecular mechanics, Huang *et al.* established a special way to decompose transfiguration energy of SWCNTs and under equivalent discrete energy models [33], the Young's modulus is reported to be about 0.361 TPa·nm. Based on analytical and structural molecular mechanics, Chang and Gao [22] and Li and Chou [16] reported Young's modulus to be 0.36 TPa·nm and 1.036 TPa respectively. In the model of Chang and Gao, carbon nanotube was supposed to be subjected to axial loadings at small strains, so the torsion, inversion, van der Waals and electrostatic interactions were ignored. In fact, in some circumstances, such as the nanotube being subjected to bending force, the torsion and inversion energy cannot be ignored. In the model of Li and Chou, the carbon-carbon bond was considered to be a beam, but the form of decomposing energy was problematical. When the carbon-carbon bond is under a bending force, it cannot express the flexibility properties the same as a macroscopic beam. There must be some modifications to represent this feature. In our model, elements of (5,5), (5,11), (6,6), (6,12), (11,5), (11,11), (12,6), and (12,12) in the sub-stiffness matrix Eq.(14) are corrected to reflect this feature.

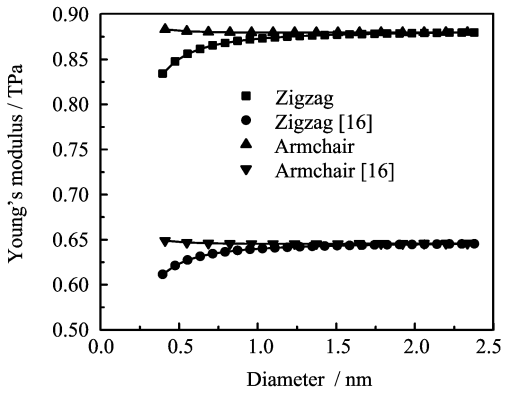

FIG. 5 Variation of Young's modulus of armchair and zigzag SWCNTs with tube radius.

Our computational results are comparable to those obtained from experiments and in reasonable agree-

DOI:10.1088/1674-0068/21/04/353-360

ment with these experimental results. Wong *et al.* obtained the Young's modulus of carbon MWCNTs of 1.28±0.59 TPa by using atomic force microscopy-based experiments [5]. The experimental data given by Krishnan *et al.* reported that the average Young's modulus is about 1.25 TPa [7]. Salvetat *et al.* reported the Young's modulus values of carbon MWNTs to be 0.81±0.41 TPa [35].

B. Shear modulus of a single-walled carbon nanotube

In the present work, a SWCNT is assumed to be subjected to forces which are tangent to the circle section on each node at one end of SWCNT and constrained at the other end. A formula based on the theory of Strength of Materials is used for obtaining the shear modulus, where the SWCNT is treated as a hollow tube with a wall thickness of 0.34 nm.

Figure 6 illustrates the computational results of shear modulus for armchair and zigzag SWCNTs. For small tube radius shear modulus increases with the tube radius; for larger radius, the shear modulus becomes insensitive to the variation of tube radius. The calculated results of shear modulus using other force field constants adopted by Li and Chou are also plotted in Fig.6 for comparison. Compared to the Young modulus, the shear modulus of SWCNT is even more sensitive to the force field constants in molecular mechanics method.

Our calculated values are comparable to the results of Lu, Popov *et al.*, Li *et al.*, and Chang *et al.* [11,16,22,29]. Using empirical lattice dynamics model, Lu reported the shear modulus about 0.5 TPa and that it is insensitive to tube radius and tube chirality. Popov *et al.* also used the lattice-dynamics model and derived an analytical expression for the shear modulus. Li applied molecular mechanics method to analyze the shear modulus of SWCNT. The results of Popov *et al.* and Li and Chou both indicated that the shear modulus of zigzag is greater than armchair for small tube radii and it increases with the tube radius for relatively small tube radius. At larger radius the shear modulus became insensitive to tube radius. The shear modulus curve of zigzag and armchair intersects as the radius of SWCNT approaches about 0.8 nm. The differences are the convergent values of shear modulus for both armchair and zigzag nanotubes. The result of Popov *et al.* is 0.398 TPa and the one of Li and Chou is about 0.475 TPa. Chang and Gao did not report shear modulus directly in their work, but using the data of Young's modulus and Poisson's ratio, the shear modulus can be deduced to a convergent value 0.431 TPa. In fact, the calculated Young's modulus and shear modulus are affected by some other factors, e.g. the length of the nanotube, and related results will be reported later on. As far as the knowledge of the present authors, no experimental shear modulus has been reported yet.

C. Poisson's ratio of single-walled carbon nanotube

Following the theory of Strength of Material, the dependence of Poisson's ratio on the tube radius can be deduced using the data of Young's modulus and shear modulus. The variation of the Poisson's ratio versus the tube radius is shown in Fig.7, together with the corresponding results given by Popov *et al.* [29]. The present values of the Poisson's ratio for armchair decreases with increasing tube radius but for zigzag it is opposite. The convergent values for both armchair and zigzag nanotubes are almost the same, around 0.27. Results given by Popov *et al.* show a similar trend. Although many investigations for Poisson's ratio of nanotubes have been conducted, there is no unique opinion that is widely accepted. Lu reported the Poisson's ratio for SWCNTs to be almost a constant of 0.28 using a force-constant model [11]. The tight-binding calculations by Goze *et al.* gave size-insensitive values of 0.247, 0.256 for (6,6), (10,10) armchair tubes and of 0.275, 0.270 for (10,0), (20,0) zigzag tubes [26]. *Ab ini-*

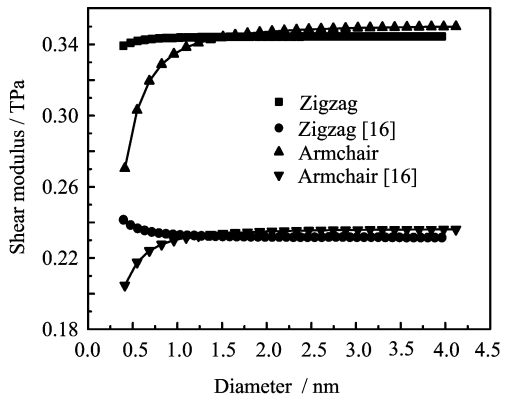

FIG. 6 Variation of shear modulus of armchair and zigzag SWCNTs with tube radius.

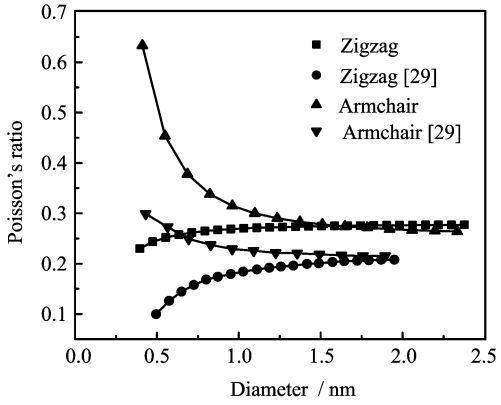

FIG. 7 Variation of Poisson's ratio of armchair and zigzag SWCNTs with tube radius

DOI:10.1088/1674-0068/21/04/353-360

tio calculations by Sanchez-Portal *et al.* showed that the Poisson's ratio for armchair tubes increases from about 0.12 to 0.16 with increasing tube size from (4,4) to (10,10) [36], while no information on the trend of the Poisson's ratio for zigzag tubes is found in the literature. Chang and Gao reported for both armchair and zigzag tubes Poisson's ratio decreased with increasing tube radius [22], it was opposite for zigzag compared to our results. In recent *ab inito* studies of Van Lier *et al.* [37], even negative Poisson's ratio is reported. Therefore, more studies will be needed in the future.

VI. DISCUSSION

We have proposed a chemical bond element model to simulate elastic properties of SWCNTs. Such a method allows us to explore nano-scale problems with the existing theory of finite element method. Building on the fundamental concepts and formulas developed here, we also plan to further develop the concept of this approach into the modeling of multi-walled carbon nanotubes (MWCNTs). The versatility of the present approach relies very much on the development of modern computational chemistry (molecular mechanics). The feasibility of applying the present approach to modeling other nanotubes would depend on the availability and accuracy of force field parameters of these materials. Compared with other refined atomistic simulation methods, such as classical molecular dynamics or tight-binding molecular dynamics, the present approach can be used for simulating both static and dynamic loadings. Also, it does not consider thermal vibration of the atoms and treats only "long time" phenomena. The economy in computation is achieved through such simplifications and the FE model performing well in a small computational time by requiring minimal computational power. This advantage, in combination with the modeling abilities of molecular mechanics method, extends the model applicability to SWCNTs with very large number of atoms as well as to MWCNTs, other carbon-related nano-structures and moreover, to CNT-based nano-composites.

We also recognize the uncertainty when a chemical bond is simply treated as a beam because the theory of structural mechanics and the theory of molecular mechanics have some different bases.

VII. CONCLUSION

A chemical bond element model has been developed for modeling SWCNTs. A simple linkage between finite element method and molecular mechanics is established. In this approach, the computational method is essentially finite element method (FEM), but the theoretical concept is considered at the nano-scale stemming from molecular mechanics. The model was used to investigate the effect of wall thickness, radius and length of SWCNT on its elastic moduli (Young's modulus and shear modulus). The FE model results suggest that Young's modulus is inversely proportional to the wall thickness.

Our computational results for elastic properties of SWCNTs are comparable to those obtained from other modeling techniques and experimental results. The major advantages of our method are the simplicity and the improved computational efficiency for analyzing the mechanical behaviors of SWCNTs. It is expected that the present methodology will be further developed to model other covalent-bonded materials and facilitate analysis of the static and dynamic properties of nanotube-based equipments.

VIII. ACKNOWLEDGMENT

This work was supported by the National Basic Research Program of China (No.2006CB300404).

[1] S. Ijima, C. Brabec, A. Maiti, and J. J. Bernholc, Chem. Phys. **104**, 2089 (1996).
[2] J. W. Mintmire, B. I. Dunlap, and C. T. White, Phys. Rev. Lett. **68**, 631 (1992).
[3] D. L. Carroll, P. Redlich, P. M. Ajayan, J. C. Charlier, X. Blase, A. DeVita, and R. Car, Phys. Rev. Lett. **78**, 2811 (1997).
[4] M. M. J. Treacy, T. W. Ebbesen, and J. M. Gibson, Nature **381**, 678 (1996).
[5] E. W. Wong, P. E. Sheehan, and C. M. Lieber, Science **277**, 1971 (1997).
[6] M. F. Yu, O. Lourie, M. J. Dyer, K. Moloni, T. F. Kelly, and R. S. Ruoff, Science **287**, 637 (2000).
[7] A. Krishnan, E. Dujardin, T. W. Ebbesen, P. N. Yianilos, and M. M. J. Treacy, Phys. Rev. B **58**, 14013 (1998).
[8] M. F. Yu, B. S. Files, S. Arepalli, and R. S. Ruoff, Phys. Rev. Lett. **84**, 5552 (2000).
[9] H. J. C. Berendsen, J. P. M. Postma, W. F. van Gunsteren, A. Dinola, and J. R. Haak, J. Chem. Phys. **81**, 3684 (1984).
[10] J. I. McKechnie, R. N. Haward, D. Brown, and J. H. R. Clarke, Macromolecules **26**, 198 (1993).
[11] J. P. Lu, Phys. Rev. Lett. **79**, 1297 (1997).
[12] N. Yao and V. Lordi, J. Appl. Phys. **84**, 1939 (1998).
[13] M. Parrinello and A. J. Rahman, J. Chem. Phys. **76**, 2662 (1982).
[14] C. Chui and M. C. Boyce, Macromolecules **32**, 3795 (1999).
[15] D. N. Theodorou and U. W. Suter, Macromolecules **19**, 139 (1986).
[16] C. Y. Li and T. W. Chou, Int. J. Solids Struct. **40**, 2487 (2003).
[17] W. S. Cho, Finite Elements in Analysis and Design **42**, 404 (2006).

DOI:10.1088/1674-0068/21/04/353-360

[18] K. I. Tserpes and P. Papanikos, Composites B **36**, 468 (2005).
[19] A. L. Kalamkarov, A. V. Georgiades, S. K. Rokkam, V. P. Veedu, and M. N. Ghasemi-Nejhad, Int. J. Solids Struct. **43**, 6832 (2006).
[20] M. Meo and M. Rossi, Comp. Sci. Technol. **66**, 1597 (2006).
[21] S. Kirtania and D. Chakraborty, J. Reinf. Plast. Compos. **26**, 1557 (2007).
[22] T. C. Chang and H. J. Gao, J. Mech. Phys. Solids **51**, 1059 (2003).
[23] T. Natsuki, K. Tantrakarn, and M. Endo, Carbon **42**, 39 (2004).
[24] J. R. Xiao, B. A. Gama, and J. W. Gillespie, Int. J. Solids Struct. **42**, 3075 (2005).
[25] T. C. Chang, J. Y. Geng, and X. G. Guo, Appl. Phys. Lett. **87**, 251929 (2005).
[26] C. Goze, L. Vaccarini, L. Henrard, P. Bernier, E. Hernandez, and A. Rubio, Synth. Met. **103**, 2500 (1999).
[27] A. K. Rappe, J. Am. Chem. Soc. **114**, 10024 (1992).
[28] Y. Q. Wang, C. J. Sun, X. K. Sun, J. Hinkley, G. M. Odegard, and T. S. Gates, Comp. Sci. Technol. **63**, 1581 (2003).
[29] V. N. Popov, V. E. Van Doren, and M. Balkanski, Phys. Rev. B **61**, 3078 (2000).
[30] B. I. Yakobson, C. J. Brabec, and J. Bernholc, Phys. Rev. Lett. **76**, 2511 (1996).
[31] G. Overney, W. Zhong, and D. Tomanek, Z. Phys. D: At. Mol. Clusters **27**, 93 (1993).
[32] E. Hernandez, C. Goze, P. Bernier, and A. Rubio, Appl. Phys. A **68**, 287 (1999).
[33] M. Y. Huang, H. B. Chen, J. N. Lu, P. Lu, and P. Q. Zhang, Chin. J. Chem. Phys. **19**, 286 (2006).
[34] J. N. Lu, H. B. Chen, P. Lu, and P. Q. Zhang, Chin. J. Chem. Phys. **20**, 525 (2007).
[35] J. P. Salvetat, J. M. Bonard, N. H. Thomson, A. J. Kulik, L. Forro, W. Benoit, and L. Zuppiroli, Appl. Phys. A **69**, 255 (1999).
[36] D. Sanchez-Portal, E. Artacho, J. M. Soler, A. Rubio, and P. Ordejon, Phys. Rev. B **59**, 12678 (1999).
[37] G. Van Lier, C. Van Alsenoy, V. Van Doren, and P. Geerlings, Chem. Phys. Lett. **326**, 181 (2000).
[38] D. Bakowies and T. Thiel, J. Am. Chem. Soc. **113**, 3704 (1991).
[39] J. M. Molina, S. S. Savinsky, and N. V. Khokhriakov, J. Chem. Phys. **104**, 4652 (1996).

DOI:10.1088/1674-0068/21/04/353-360